DOI:10.5937/IIZS26425J

ANALYSIS OF AIR POLLUTION SPATIAL DISTRIBUTION: DISPERSION MODEL WITH MULTILAYER ATMOSPHERIC STRUCTURES (DMMAS)

Research paper

Stevo K. Jaćimovski[1], Dane Subošić[2], Dušan I. Ilić[3], Jovan P. Šetrajčić[4,*]

[1,2]University of Criminal Investigation and Police Studies, Zemun – Belgrade, Serbia;
[3]University of Novi Sad, Technical Faculty, Novi Sad, Vojvodina – Serbia;
[4]Academy of Sciences and Arts of the Republic of Srpska, Banja Luka, B&H.

Abstract: This paper presents the results of a semi-analytical solution to the two-dimensional, time-dependent advection-diffusion equation, based on the discretization of the surface boundary layer (SBL) into *N* sub-layers. Within each sub-layer, the equation is solved using Laplace transforms, incorporating mean values for the turbulent diffusion coefficient and wind speed. The actual pollutant concentration is determined by numerically calculating the inverse Laplace transform via the Gaussian quadrature method. The pollutant concentration distributions obtained through this approach are compared with those from the Gaussian atmospheric dispersion model, as well as with available experimental results.
Key words: DMMAS model, inverse Laplace transforms, diffusion coefficient, wind speed, Gaussian quadrature, Gaussian model.

INTRODUCTION

Recently, a semi-analytical solution of the advection-diffusion equation for non-stationary conditions was obtained (Vilhena, et al. 1998). From this solution, a model named AMMD (Analytical Model of Multilayer Dispersion) was set up. The model is based on the discretization of the PBL (Planetary Boundary Layer) into *N* sub-layers, where in each sub-layer the advection-diffusion equation is solved using the Laplace transform technique, taking into account the average value of turbulence and wind speed. The main feature of this method is based on the following steps: stepwise approximation of turbulence and wind speed, double Laplace transformation for the advection-diffusion equation in *x*, *z* and *t* variables, semi-analytical solution of a set of linear ordinary equations resulting from the application of double Laplace transformation and construction of pollutant concentration using the inverse Laplace transformation using the so-called Gauss quadrature scheme (Moreira, et al., 2005). The model represents a semi-analytical solution due to the numerical inversion of the Laplace transform of the solution of the advection-diffusion equation.

DMMAS MODEL

The equation of advection and diffusion that describes the temporal evolution of the concentration of *C*, due to the release of the amount of polluting material continuously in time by an elevated source placed at (0,0,*h*), in a horizontally homogeneous atmosphere is (Tirabasi, T. et al., 2010):

$$\frac{\partial C}{\partial t} + u\,\frac{\partial C}{\partial x} = \frac{\partial}{\partial z}\left(K_z\,\frac{\partial C}{\partial z}\right). \tag{1}$$

The mathematical description of the dispersion problem represented by equation (1) is well defined when the initial and boundary conditions are provided. Indeed, it is assumed that at the beginning of the pollutant release, the dispersion region is not polluted, which means that:

[1]jacimovskis@gmail.com, ORCID No: 0000-0002-4074-662X.
[4]Corresponding author, jovan.setrajcic@gmail.com, ORCID:0000-0002-6903-2882

$$C(x,z,0) = 0, \text{ at } t = 0. \quad (2)$$

At the point (0,*z*,*t*), a continuous line source with a constant emission rate *Q* is assumed, i.e.

$$u\,C(0,z,t) = Q\,\delta(z-h), \quad \text{at } x = 0, \quad (3)$$

where *δ* is the Dirac delta function and h is the height of the source. Pollutants are also subject to zero flux boundary conditions at the ground and top of the PBL. The PBL is the boundary layer of the atmosphere (BLA), and it is covered by the inversion layer, so that within the inversion layer the atmosphere becomes extremely stable and there is no mixing of pollutants. Inverse conditions in the atmosphere (temperature inversion) represent the phenomenon when the air temperature increases with the increase in altitude, which is the opposite of the usual state in the troposphere where the temperature decreases. This condition in the atmosphere causes a stable air layer that prevents vertical mixing, which often leads to the retention of cold air, fog and pollutants in the lower layers. The inversion at the top of the PGS practically acts as an impermeable surface, and the boundary condition applies to it:

$$K_z \frac{\partial C}{\partial z} = 0, \quad \text{at } z = 0, H. \quad (4)$$

Here, *H* is the height of the boundary layer of the atmosphere. Experimental determination of the height of the boundary layer is very complex and can be carried out using radiosondes, weather balloons, towers, aircraft, radar and other methods. Given that experimental values are often unavailable, mathematical modeling is used to obtain mixing height values (Pocajt, 2018). The height of the inversion layer depends on several parameters and has different values for different conditions of atmospheric stability.

The reliability of the model largely depends on how the dispersion parameters are determined based on the structure of the (PBL) turbulence and the ability of the model to reproduce experimental diffusion data. There are a large number of formulations for the dispersion coefficient and wind speed, and the paper will use Degrazie's formulation (Degrazia, G.A. & Moraes, O.L.L., 1992; Degrazia, G.A. et al., 2001):

$$K(z) = 0{,}22\,u_*\,H\,\left(\frac{z}{H}\right)^{\frac{1}{3}}\left(1-\frac{z}{H}\right)^{\frac{1}{3}}\left[1-\exp\left(-\frac{4z}{H}\right)-0{,}0003\exp\left(\frac{8z}{H}\right)\right]; \quad (5)$$

$$u(z) = \frac{u_*}{k}\left[\ln\frac{z}{z_0} - \Psi_m\left(\frac{z}{L}\right) + \Psi_m\left(\frac{z_0}{L}\right)\right], \quad (6)$$

where is:

$$\Psi_m = 2\ln\left[\frac{1+A}{2}\right] + \ln\left[\frac{1+A^2}{2}\right] - 2\arctan A + \frac{\pi}{2};\ \ A = \left(1-16\,\frac{z}{L}\right)^{\frac{1}{4}}. \quad (7)$$

Since both mechanical and convective forces determine turbulence, Monin and Obukhov (Monin, A.S. & Obukhov, A.M., 1953) proposed a similarity theory that introduced two scaling parameters: the friction velocity u_* and the Monin-Obukhov length (*L*), which is a measure of the depth of the surface layer in which shear effects are significant under any conditions of atmospheric stability (Esmail, S.F.H., 2011), and is expressed (Ilijazi, V., 2022) as:

$$L = -\frac{u_*^3 c_p Q T}{g k G}, \tag{8}$$

where c_p is the specific heat of air at constant pressure, Q air density, k von Karman constant, T air temperature, g gravitational acceleration and G heat flux. For unstable, neutral and stable conditions, the values of L are less than zero, equal to 0 and greater than zero, respectively (Esmail, S.F.H., 2011).

Taking into account the dependence of the coefficient $K(z) \rightarrow K_z$ and the wind speed profile u on the variable z, the height of the PGS is discretized in N sub-intervals (as in the sketch from Figure 1) in such a way that within each interval K_z and u $u(z) \rightarrow u_z$ assume mean values:

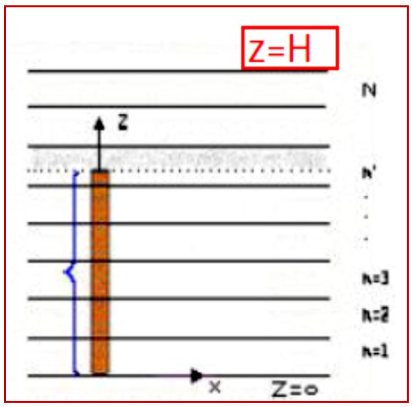


Fig. 1. *Schematic representation of the discrete layering of the dispersion coefficient and velocity along the z-direction*

$$K_n = \frac{1}{z_{n+1}-z_n} \int_{z_n}^{z_{n+1}} K_n(z)\, dz; \tag{9}$$

$$u_n = \frac{1}{z_{n+1}-z_n} \int_{z_n}^{z_{n+1}} u_n(z)\, dz. \tag{10}$$

Therefore, based on that, the solution of equation (1) is reduced to the solution of N problems of this type:

$$\frac{\partial C_n}{\partial t} + u_n \frac{\partial C_n}{\partial x} = K_n \frac{\partial^2 C_n}{\partial z^2}, \tag{11}$$

for n = 1, 2, 3, ⋯, N – 1, where C_n denotes the concentration in the nth subinterval. In order to determine the 2N integration constants, additional 2N – 2 conditions are considered, such as the continuity of concentration and flow at the boundaries in the following form:

$$C_n = C_{n+1}, \quad \text{for} \quad n = 1,2,\ldots,(N-1); \tag{12}$$

$$K_n \frac{\partial C_n}{\partial z} = K_{n+1} \frac{\partial C_{n+1}}{\partial z}, \quad \text{for} \quad n = 1,2,\ldots,(N-1). \tag{13}$$

By applying the Laplace transformation to (11), we get:

$$\frac{\partial^2 \bar{C}_n(s,z,p)}{\partial z^2} - \frac{p+su_n}{K_n} \bar{C}_n(s,z,p) = -\frac{u_n}{K_n} \bar{C}_n(0,z,p), \tag{14}$$

where: $\bar{C}_n(s,z,p) = L\{C_n(x,z,t;\ x \rightarrow s;\ t \rightarrow p\}$ – Laplace figure of concentration in sublayer n. The solution of equation (14) is known (Tošić,B.S., et al., 2018) and is expressed in the following form:

$$\bar{C}_n(s,z,p) = A_n e^{-R_n z} + B_n e^{R_n z} + \frac{Q}{2R_a}\left[e^{-R_n(z-H)} - e^{R_n(z-H)}\right], \tag{15}$$

where are:

$$R_n = \sqrt{\frac{(p+s\,u_n)}{K_n}}; \quad R_a = \sqrt{(p+s\,u_n)K_n}. \tag{16}$$

Applying the initial and boundary conditions, a system of linear algebraic equations for the integration constants A_n and B_n is obtained, as in (Essa, K.S.M. & Taha H.M.A., 2023):

$$A_n = B_n = \frac{Q\left[\mathrm{e}^{R_n(H-h)}+\mathrm{e}^{-R_n(H-h)}\right]}{2R_a(\mathrm{e}^{R_nH}-\mathrm{e}^{-R_nH})}. \tag{17}$$

After that, the concentration is obtained by numerically inverting the transformed concentration C_n using the Gauss quadrature method (Moreira, et al., 2005) in the following form:

$$C_n(x,z,t) = \sum_{i=1}^{k} w_i\left(\frac{P_i}{t}\right)\sum_{j=1}^{M} w_j\left(\frac{P_j}{t}\right)\Bigg\{A_n\,\mathrm{e}^{-\sqrt{\frac{P_j}{tK_n}+\frac{P_ju_n}{xK_n}}(z-h)} - B_n\,\mathrm{e}^{\sqrt{\frac{P_j}{tK_n}+\frac{P_ju_n}{xK_n}}(z-h)} + \\ + \frac{1}{2}\frac{Q}{2\sqrt{\frac{P_jK_n}{t}+\frac{P_ju_nK_n}{x}}}\left[\mathrm{e}^{-\sqrt{\frac{P_j}{tK_n}+\frac{P_ju_n}{xK_n}}(z-h)} - \mathrm{e}^{\sqrt{\frac{P_j}{tK_n}+\frac{P_ju_n}{xK_n}}(z-h)}\right]\theta(z-h)\Bigg\}. \tag{18}$$

Here $\theta(z-H)$ is the Heaviside function defined, e.g. as in [Tošić, B.S., et al., 2018]:

$$\theta(z-h) = \begin{cases} 1, & \text{za } z > h; \\ 0, & \text{za } z < h, \end{cases} \tag{19}$$

which indicates that the second term in (18) is added only for $z > h$.
Gauss-Lager integration (Stroud, & Secrest D., 1996) is an approximate method for finding the numerical value of the Laplace transform:

$$\int_0^\infty f(\mathrm{p})dp = \int_0^\infty \mathrm{e}^{-p}[e^p f(p)]\;dp \approx \sum_{j=1}^{n} w(p_j)\;\mathrm{e}^{p_j} f(p_j), \tag{20}$$

where p_j are the values of the roots of Lager polynomials of the appropriate degree (Tošić, B.S., et al., 2018). With this, the values of the corresponding variables, usually: $k = 2$, $M = 8$, (Stroud, & Secrest D., 1996) for the integration procedure defined in (18) are calculated and shown in Table 1. Adopted values of parameters for calculating pollutant concentration according to (Moura A.B.D., 2018) are:

L = 116 m, Q = 400 g/m2, H = 400 m, u_* = 0,31 m/s, h = 12,5 m, z_0 = 0.6 m, t = 7.200 s.

Table 1. *Values of the roots of the Lager polynomials and the corresponding weighting factors for the application of Gauss-Lager quadrature methods*

No. i	Root of a Laguerre polynomial, of order i, p_i	Weight factor $w(p_i)$	Total weight factor, $w(p_i)\;\mathrm{e}^{p_i}$
1	0,585786	0,853553	1,53333
2	3,414210	0,146447	4,45096
No. j	Root of a Laguerre polynomial, of order j, p_j	Weight factor, $w(p_j)$	Total weight factor, $w(p_j)\mathrm{e}^{p_j}$

1	0,170280	0,36918900	0,437723
2	0,903702	0,41878700	1,033870
3	2,251090	0,17579500	1,669710
4	4,266700	0,03334350	2,376920
5	7,045910	0,00279454	3,208540
6	10,758500	$9{,}07651 \cdot 10^{-5}$	4,268580
7	15,740700	$8{,}48575 \cdot 10^{-7}$	5,818080
8	22,863100	$1{,}04800 \cdot 10^{-9}$	8,906230

Based on all that, the dependence of the diffusion coefficient on the height was calculated numerically and is shown graphically in Figure 2.

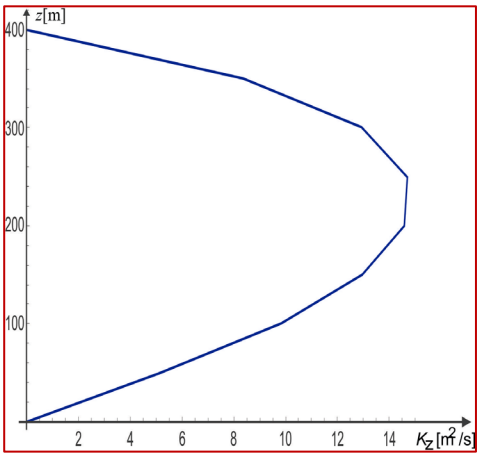


Fig. 2. *Dependence of the diffusion coefficient on the height z according to relation (5) →*

Figure 2 clearly shows the complex dependence of the diffusion coefficient with increasing distance from the earth's surface. This dependence is much more adapted to real atmospheric conditions and stability classes than the situation and the complex relationship of advective and diffuse flow.

In the Gaussian model, the diffusion coefficient is assumed to depend on x, for example, as a power function. Similar considerations apply to the dependence of wind speed u, defined by relations (6) and (7).

As an example of using the DMMAS model, it was adopted that the atmosphere from the surface to the PGS layer is divided into four layers with heights: Δz_1= 12,5 m (from the ground surface to the height of the source), Δz_2= 67,5 m; Δz_3= 120 m and Δz_4= 200 m. For those layers, according to (5), (6) and (7), and according to relation (10), the corresponding mean values of diffusion coefficients K_1, K_2, K_3, K_4 and mean values of wind speeds u_1, u_2, u_3, u_4 are found. According to (17) and the found mean values of the diffusion coefficient and the mean values of the wind speeds by layers, the values of the coefficients R_1, R_2, R_3, R_4 and R_{a1}, R_{a2}, R_{a3}, R_{a4} are found. For the given adopted parameters and for the case of a neutral or stable atmosphere and with the use of data from table 1 according to relation (18), the concentrations of air pollutants at the height z = 100 m (third layer) and z = 300 m (fourth layer) along the distance x ϵ (0, 12 km) were sought. This x-axis distance was chosen in order to be able to compare the results with the results within the Gaussian model, which gives valid results up to these distances. A graphical presentation of the results is given in Figure 3.

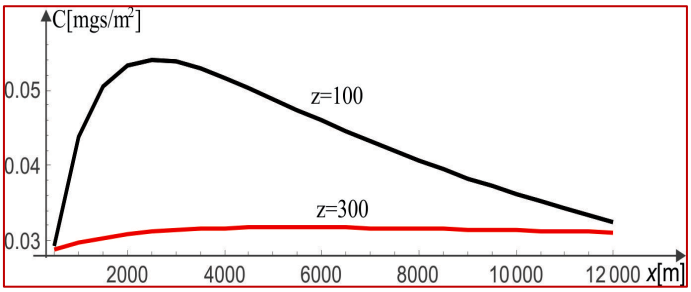


Fig. 3. *Comparative presentation of the distribution of pollutants at different heights, according to the DMMAS model*

From Fig. 3, it is noticeable that the concentration of pollutants is higher at lower altitudes and vice versa, which is again in accordance with physical laws.

GAUSS MODEL

The Gaussian model of the spatial distribution of air pollutants is the most commonly used analytical-mathematical model in environmental protection engineering and meteorology for estimating the distribution and concentration of pollutants in the atmosphere. The model observes a stationary point source (e.g. a factory chimney) from which GSAs are emitted at a constant rate. The smoke plume travels downwind, while turbulent diffusion spreads it laterally – horizontally and to the height – vertically (Nikezić, D.P., 2016), which is shown in Fig. 4.

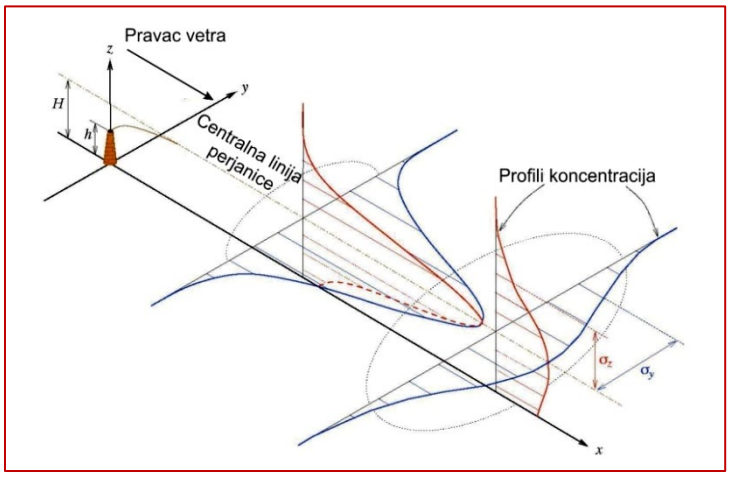


Fig. 4. *Distribution of pollutants according to the Gaussian model*

The expression for the concentration in the Gaussian model, with the reflection of pollutants from the earth's surface, according to (Vulović, A., 2022), has the following form:

$$C(t,x,z) = \frac{Q}{2\pi u \sigma_y(x)\sigma_z(x)} \exp\left(-\frac{(x-u\,t)^2}{2\sigma_x^2(x)}\right)\left\{\exp\left[-\frac{(z-l)^2}{2\sigma_z^2(x)}\right] + \exp\left[-\frac{(z+l)^2}{2\sigma_z^2(x)}\right]\right\};$$
$$\sigma_y = ax^b; \qquad \sigma_z = cx^d, \tag{21}$$

where *a*, *b*, *c*, *d* are the empirical coefficients, which depend on the stability class of the atmosphere and whose values are given in table 2. The wind speed at height l is determined by the expression:

$$\bar{u}(l) = u(z_1)\left(\frac{l}{z_1}\right)^m, \tag{22}$$

where z_1 is a fixed height, and *m* is an exponent that depends on the class of atmospheric stability (Table 2).

Table 2. *Pasquila stability classes and empirical coefficients*

	a	***b***	***c***	***d***	***m***
A	0,235	0,796	0,311	0,711	0,53
B	0,297	0,796	0,382	0,711	0,40
C	0,418	0,796	0,520	0,711	0,33

D	0,586	0,796	0,700	0,711	0,23
E	0,826	0,796	0,950	0,711	0,16
F	0,946	0,796	0,321	0,711	0,10
G	1,043	0,698	0,819	0,669	0,33

Applying relations (21) and (22), taking the points from Table 2, for the neutral atmospheric class of stability, the distribution of air pollutants at the height of z = 300 m is found, the graphic representation of which is given in Figure 5.

If we compare the obtained data on the distribution of air pollutants for the same parameter values and the same stability class in the Gaussian and DMMAS models and show it graphically (Figure 6), a drastic difference is obtained.

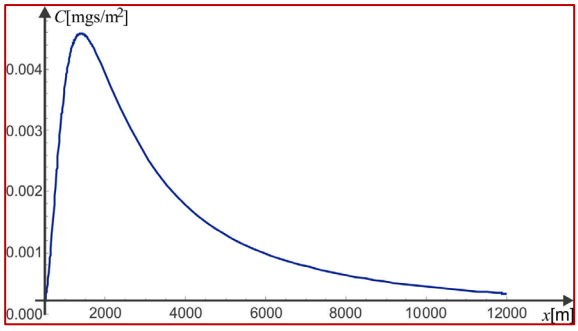


Fig. 5. *Gaussian distribution of air pollutants in space*

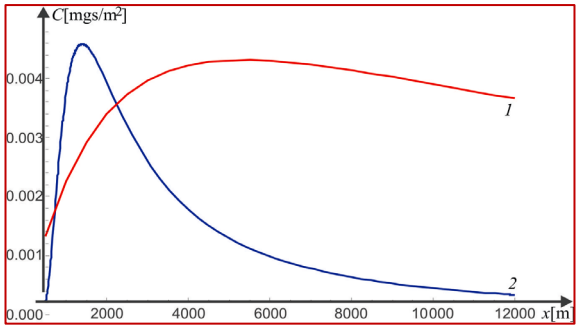


Fig. 6. *Comparative presentation of the distribution of pollutants for the same parameter values and the same class atmospheric stability: 1 – DMMAS model; 2 – Gaussian model*

From Figure 6, it can be seen that the Gaussian model gives a slightly higher maximum pollutant concentration value of 0,00455 mg/m^2 and that they are closer to the source (at 1.500 m) than the values predicted by the DMMAS model of 0,00455 mg/m^2 (at 5.500 m). At the same time, the DMMAS model indicates that pollutant concentrations do not decrease sharply with distance, after reaching the peak, i.e. maximum values.

VALIDATION OF RESULTS

Model verification is an assessment of the practical value and accuracy of the model. There is general agreement that experimental data, and especially field measurements, are the main criteria for model verification. Despite that fact, model verification is an extremely complex problem. The reasons for that are as follows (Pocajt, V. & Antanasijević D., 2018):

- The appropriate assessment method cannot be defined in a unique way, since the methods used depend on the context of application;
- Experimental field data sets for evaluation are limited and reflect only a small part of the possible scenarios. For a correct assessment of the model, it is necessary to use as many data sets as possible, with an understanding of the nature of the model;

During 1987, an experiment was conducted in Copenhagen in which SF_6 concentration values were measured in a certain period of time for different classes of atmospheric stability (Gryning, S.E., et al., 1987). This experiment serves to check the validity of DMMAS and the Gaussian model. According to Hanna (Hanna, S.R., 1989), the statistical parameters necessary for comparing the quality of the model with experimentally determined normalized concentrations are:

- Normalized mean square error: $NMSE = \frac{\overline{(C_M - C_R)^2}}{\overline{C_M}\ \overline{C_R}}$;

- Linear correlation coefficient: $R = \frac{\overline{(C_M - \overline{C_M})(C_R - \overline{C_R})}}{\sigma_{C_M}\sigma_{C_R}}$;

  (The coefficient of linear correlation (*R*) provides the least information, and thus is the least significant, of the displayed statistical indicators, because it represents the degree of linear correlation of predicted and correct values.)
- Proportion of correct predictions: $FAC2\colon\ 0{,}5 \leq \frac{C_R}{C_M} \leq 2{,}0$;

  (The proportion of correct predictions relative to the correct value. The *FA* indicator is one of the most significant statistical indicators of the model's performance, because it shows the model's ability to provide accurate predictions for a certain resolution of the error, for each individual examined case. *FAC2* shows the proportion of predictions with a relative error of less than ± 20 % allows the models to be effectively classified by performance, depending on the complexity of the problem and the required accuracy.)
- Fractional tendency: $FB = \frac{(\overline{C_M} - \overline{C_R})}{0{,}5(\overline{C_M} + \overline{C_R})}$,

  where: C_M – measured concentration and C_R – concentration calculated according to the appropriate model, and the line above the appropriate size indicates the arithmetic mean value of the given size.

If the model were perfect, i.e. if the calculated results matched the measured values, the *R* and *FAC*2 parameters would have a value of 1, and the *MNSE* and *FB* parameters would have a value of 0. Such matching is only possible in an ideal situation because no model is perfect. Table 3 shows the comparative values of the statistical parameters of the measured normalized concentrations and their values for the case when the normalized concentrations are calculated using different models.

Table 3. *Comparison of calculated values based on DMMAS and Gaussian model*

Modeli	***NMSE***	***R***	***FAC2***	***FB***
DMMAS	0,10	0,91	1,00	0,16
Gaussian	0,58	0,80	0,59	0,58

According to Table 3, it is obvious that the DMMAS model predicts the values of air pollutant concentrations significantly better than those predicted by the Gaussian model.

CONCLUSIONS

The aim of this paper was to present and discuss the results of the comparison between the Gaussian model and the DMMAS model based on the time-dependent semi-analytical solution of the advection-dispersion equation for the simulation of pollutant propagation in SBL. For a better understanding of the comparison between the two models in this paper, the focus is on the mathematical characteristics of the two approaches. Regarding the DMMAS method, it is important to emphasize that no approximation is made in this approach except the approximation of the meteorological parameters by layers and Laplace numerical inversion using the Gaussian quadrature scheme. In the DMMAS method, it is only necessary to choose the number of sublayers appropriately, taking into account the smoothness of the functions Kz and u (Moreira, D.M., et al., 2005).

The advantage of the Gaussian model lies in its exceptional computational simplicity, fast analytical results and the possibility of insight into the spatial distribution of pollution based on minimal input meteorological data. This is why it forms the basis of many modern modeling software packages (Aermod, Calpuff, ...). However, the Gaussian model does not give good results in conditions of complex topography (mountains, valleys), with extremely weak winds < 1 m/s, as well as for reactive pollutants that enter into photochemical reactions in the atmosphere (Hanna, S.R., et al., 1989).

With the same input values of the model parameters, the same atmospheric stability classes, both models give approximately the same maximum concentration values, at approximately the same distance from the source. However, the DMMAS model indicates significantly higher concentrations of air pollutants at greater distances from the source (Figure 5). In addition, according to the statistical characteristics of the validation of the DMMAS model, the model is more consistent than the Gaussian model with the experimentally measured values of air pollution.

REFERENCES

Degrazia, G.A., Moraes, O.L.L. (1992). A Model for Eddy Diffusivity in a Stable Boundary Layer, *Boundary-Layer 0 Meteorology* **58**, 205-214.

Degrazia, G.A., Moreira, D.M., Vilhena, M.T. (2001). Derivation of an Eddy Diffusivity Depending on Source Distance for Vertically Inhomogeneous Turbulence in a Convective Boundary Layer, *J. Appl. Meteor.* **40**, 1233–1240.

Essa K.S.M., Taha H.M.A. (2023). Studying the Effect of Two Analytical Solutions of Advection-Diffusion Equation on Experimental Data, *Pure Appl. Geophys*. **180**, 2407–2418.

Esmail S.F.H. (2011). Assessment of Concentration of Air Pollutants Using Analytical and Numerical Solutions of the Atmospheric Diffusion Equation, Thesis, *Faculty of Science, Zagazig University*.

Gryning S.E., Holtslag A.A.M., Irwin J.S., Siversten B., (1987). Applied Dispersion Modelling Based on Meteorological Scaling Parameters, *Atmos. Environ.* **21**/1, 79-89.

Hanna S.R. (1989). Confidence Limits for Air Quality Model Evaluations, as Estimated by Bootstrap and Jackknife Resampling Methods. *Atmos. Environ.* **23**, 1385-1398, doi: 10.1016/0004 6981(89)90161-3.

Hanna, S.R., Briggs, G.A., Jr. Hosker, R.P. (1982). Handbook on Atmospheric Diffusion. Prepared for the Office of Health and Environmental Research, office of Energy Research, *U.S. Department of Energy*, DOE/TIC 11223, J.S. Smith, Publ. Ed.

Ilijazi V. (2022), Modeling the distribution of air pollutants in accidents as a function of IT support for early response, Dissertation, *University of Criminal Investigation and Police Studies,* Zemun – Belgrade – in Serbian.

Moreira D.M., Neto P.V.F., Carvalho J.C., (2005). Analytical Solution of the Eulerian Dispersion Equation for Nonstationary Conditions: Development and Evaluation, *Environmental Modelling and Software*, **20**/9, 1159-1165.

Monin A. S., Obukhov A. M., (1953). *Doklady Akad. Nauk USSR* **93**, 2 – In Russian.

Moura, A.B.D. (1995). Analytical Solution of Turbulent Vertical Dispersion in the Stable Boundary Layer. Dissertation, *Federal University of Rio Grande do Sul*.

Nikezić, D.P. (2016). Mathematical Modeling of the Spread of Pollutants in the Air in the Vicinity of Nuclear and Industrial Facilities, Doctoral Dissertation, *Faculty of Technological Metallurgy, University of Belgrade*, Belgrade – in Serbian.

Pocajt, V., Antanasijević, D. (2018). Selected Chapters in Life Protection Engineering Environment, *Faculty of Technology and Metallurgy, University of Belgrade*, Belgrade – in Serbian.

Stroud A. H., Secrest D., (1996). Gaussian Quadrature Formulas, *Prentice-Hall*, Englewood Cliffs, p. 320.

Tirabassi T., Moreira D.M., Vilhena M.T, da Costa C.P.,(2010), Comparison between Non-Gaussian Puff Model and a Model Based on a Time-Dependent Solution of Advection-Diffusion Equation, J*. Environ. Protection* **1**, 172-178.

Tošić B.S., Šetrajčić J.P., Jaćimovski S.K., (2018). Methods of Theoretical Physics, *University of Criminal Investigation and Police Studies,* Zemun – Belgrade – in Serbian.

Vilhena, M.T., Rizza, U., Degrazia, G.A., Mangia, C., Moreira, D.M., & Tirabassi, T. (1998). An Analytical air Pollution Model: Development and Evaluation. *Contr. Atmos. Phys*. **71**/3, 315–320.

Vulović A. (2022), Analysis of the Impact of Air Pollutants on Human Health from the Aspect of Environmental Forensics, Dissertation, *University of Criminal Investigation and Police Studies,* Zemun – Belgrade – in Serbian